



# Effect of prolonged electrode potential cycling on the charge transport parameters of poly(o-aminophenol) films. A study employing rotating disc electrode voltammetry and surface resistance



Ricardo Tucceri\*

Instituto de Investigaciones Fisicoquímicas Teóricas y Aplicadas (INIFTA), CONICET, Facultad de Ciencias Exactas, Universidad Nacional de La Plata, Sucursal 4, Casilla de Correo 16, 1900 La Plata, Argentina

## ARTICLE INFO

### Article history:

Received 28 October 2013

Accepted 13 January 2014

Available online 23 January 2014

### Keywords:

Poly(o-aminophenol) film electrodes

Prolonged potential cycling (PPC)

Deactivation

Electron diffusion coefficient

Surface resistance

## ABSTRACT

The aim of this work was to study the effect of prolonged potentiodynamic cycling (PPC) on the conducting properties of poly(o-aminophenol) (POAP) film electrodes. Cyclic Voltammetry (CV), Rotating Disc Electrode Voltammetry (RDEV) and Surface Resistance (SR) were employed in this study. The attenuation of the voltammetric response of the polymer with the increase in the number of oxidation–reduction cycles allowed one to define a degree of deactivation. RDEV was employed to obtain the dependence of the electron diffusion coefficient on the degree of deactivation of the polymer. The slower electron transport with the increase in the degree of deactivation was attributed to the increase of the electron hopping distance between redox sites. The attenuation of the relative resistance changes ( $\Delta R/R$ ) of a gold film coated with a POAP film as the degree of deactivation increases was also associated to changes in the redox site configuration at the gold/POAP interface after PPC. POAP films maintain their conducting properties almost unaltered for about 500 potential cycles at a scan rate of  $0.010 \text{ V s}^{-1}$ . However, a loss of conductivity was observed as the number of potential cycles was extended beyond 500.

© 2014 Elsevier B.V. All rights reserved.

## 1. Introduction

The oxidation of o-aminophenol (o-AP) on different electrode materials (gold, platinum, carbon, indium–tin oxide, etc.) in aqueous medium was shown to form poly-o-aminophenol (POAP) [1–3]. O-AP can be polymerized electrochemically in acidic, neutral and alkaline solutions. While a conducting film is only formed in acidic media, POAP synthesized in neutral and alkaline media leads to a nonconducting film [4,5]. The charge-transport process at POAP films synthesized in acid medium was mainly studied from the basic research viewpoint employing different electrochemical techniques [1,3,6,7]. POAP synthesized in acidic medium is also found to be a useful material to build electrochemical sensors and electrocatalysts [8–11]. Considering the interest in POAP synthesized in acid medium in both basic and applied research, no much attention has been paid to the decay of the electroactivity of POAP caused by its extensive use. The aim of the present work is to study how the charge-transport process of POAP changes with PPC. Three techniques were employed in this work: Cyclic Voltammetry (CV), Rotating Disc Electrode Voltammetry (RDEV) and Surface Resistance (SR) [12–14]. CV was employed to assess a degree of deactivation. RDEV data were analyzed in terms of the electron

hopping model [15]. The objective of the interfacial resistance measurements was to demonstrate the existence of different distributions of redox sites at deactivated POAP film electrodes as compared with nondeactivated ones. It is expected that the present work will shed light on the limits of stability and durability of POAP, particularly when it is proposed as material to develop sensors and electrocatalysts.

## 2. Experimental

### 2.1. CV and RDEV measurements

A gold rotating disc electrode (RDE) was used as base electrode to deposit POAP films. This gold RDE consisted of a gold rod press-fitted with epoxy resin into a Teflon sleeve so as to leave a  $1 \text{ cm}^2$  disc area exposed. The electrode was carefully polished with emery paper of decreasing grit size followed by alumina suspensions of 1, 0.3 and  $0.05 \mu\text{m}$ , respectively, until a mirror-like finish was obtained. Then, it was submitted to ultrasonic cleaning to remove residual abraded polishing material. In order to obtain a more specular gold surface to deposit POAP films, a gold film about 50 nm in thickness was deposited by vacuum evaporation [12,13,16] ( $\sim 10^{-7}$  Torr) on the gold disc. The thickness of the evaporated gold thin film was determined as described in [14,16]. Then, in all experiments carried out in this work, POAP films were

\* Tel.: +54 0221 425 7430; fax: +54 0221 425 4642.

E-mail address: [rtucce@inifta.unlp.edu.ar](mailto:rtucce@inifta.unlp.edu.ar)

deposited on a specular gold film surface. POAP films were grown on these base electrodes following the procedure described in [1,2]. That is, polymer films were obtained by immersing the base electrode in a  $10^{-3}$  M *ortho*aminophenol + 0.4 M  $\text{NaClO}_4$  + 0.1 M  $\text{HClO}_4$  solution and cycling the potential between  $-0.25$  and  $0.8$  V (versus SCE) at a scan rate  $\nu = 0.05$   $\text{V s}^{-1}$ . In the same way as in [6,15,17,18], POAP films were grown up to an approximate thickness of  $\phi_p \sim 60$  nm by using a reduction charge ( $Q_{\text{Red,T}} = 2.8$   $\text{mC cm}^{-2}$ ) versus the ellipsometric thickness working curve [17]. These POAP-coated gold film electrodes were then rinsed and transferred to the supporting electrolyte solution (0.4 M  $\text{NaClO}_4$  + 0.1 M  $\text{HClO}_4$ ) free of monomer, where they were stabilized by a continuous potential cycling at a scan rate of  $0.01$   $\text{V s}^{-1}$ . A typical voltammetric response of these films is shown in Fig. 1 (plot (a)). The POAP films maintain this response on potential cycling within the potential range  $-0.2$  V  $< E < 0.5$  V up to 500 cycles. These POAP films are herein called nondeactivated films. A large-area gold grid was used as counterelectrode. All the potentials reported in this work are referred to the SCE.

A series of eight POAP-coated RDE was prepared (see first column in Table 1) and each one of them was successively employed in an individual experiment. That is, each POAP film was subjected to a different number of potential cycles (higher than 500 cycles, see second column in Table 1) within the potential region  $-0.2 < E < 0.5$  V in a deoxygenated supporting electrolyte solution. Then, the corresponding  $j$ - $E$  responses for each one of the eight POAP films were recorded. An attenuation of the voltammetric response was observed for these films when the number of potential cycles was higher than 500 (Fig. 1). These POAP films are herein called deactivated films. Then, with both nondeactivated and deactivated POAP films, RDEV were performed in the presence of a solution containing equimolar concentrations of *p*-benzoquinone (Q) and hydroquinone (HQ) species (0.1 M  $\text{HClO}_4$  + 0.4 M  $\text{NaClO}_4$  +  $2 \times 10^{-3}$  M Q/HQ). Stationary current-potential curves ( $I$ - $E$ ) at different electrode rotation rates,  $\Omega$ , were recorded. From these curves, cathodic and anodic limiting current versus electrode rotation rate ( $I_{\text{lim}}$  versus  $\Omega^{1/2}$ ) dependences were obtained. In some experiments the HQ/Q redox couple concentration in solution was varied.

In CV and RDEV measurements a PAR Model 173 potentiostat and a PAR Model 175 function generator were used. An X1-X2-Y Hewlett-Packard Model 7046 B plotter was used to record  $j$ - $E$  and steady-state current-potential curves  $I$ - $E$ . The electrode rotation speed,  $\Omega$ , was controlled with homemade equipment that allows one to select a constant  $\Omega$  in the range  $50$   $\text{rev min}^{-1} < \Omega < 7000$   $\text{rev min}^{-1}$ . This was periodically controlled with a digital photo tachometer (Power Instruments Inc., model 891).

AR grade chemicals were used throughout. *O*-aminophenol (Fluka) was purified as described elsewhere [1,2].  $\text{HClO}_4$  and  $\text{NaClO}_4$  (Merck) were used without further purification. Benzoquinone and hydroquinone (Merck) were also used without purification. The solutions were prepared with water purified using a Millipore Milli-Q system.

## 2.2. Surface resistance measurements

The arrangement employed to perform SR experiments is one in which a POAP film is supported on a rectangular thin gold film. Eight gold thin film electrodes of constant thickness  $\phi_m \sim 30$  nm were prepared by vacuum evaporation as was previously described [12,13,16]. All these electrodes exhibit initial resistance ( $R$ ) values of about  $20.02 \Omega$ . The relationship between the length,  $l$ , and the width,  $w$ , ( $G = l/w$ ) of these gold film electrodes was 2.043. The electrode area was  $1$   $\text{cm}^2$ . POAP films of 60 nm thickness were grown on these base electrodes following the procedure previously described. A series of eight POAP-coated gold film electrodes was

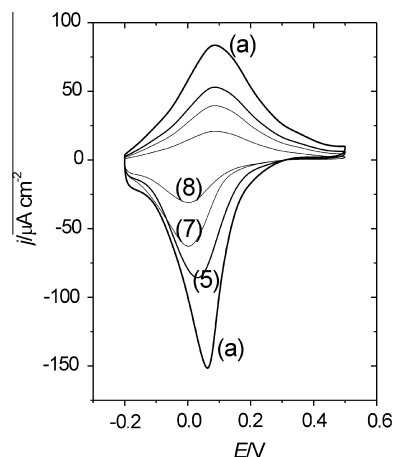


Fig. 1. Voltammetric ( $j$ - $E$ ) responses for a  $2.8$   $\text{mC cm}^{-2}$  ( $\phi_p = 60$  nm) thick POAP film. (a) A nondeactivated POAP film ( $\theta_c^d = 0$ ). Curves (5), (7) and (8) correspond to films whose degree of deactivation is:  $\theta_c^d = 0.42$ ;  $\theta_c^d = 0.62$  and  $\theta_c^d = 0.74$ , respectively. Electrolyte:  $0.1$  M  $\text{HClO}_4$  +  $0.4$  M  $\text{NaClO}_4$ . Scan rate:  $\nu = 0.01$   $\text{V s}^{-1}$ .

Table 1  
Effect of the prolonged potential cycling on the voltammetric charge of a POAP film.

<sup>a</sup> POAP films	<sup>b</sup> Number of potential cycles	<sup>c</sup> $Q_{\text{Red,c}}$ ( $\text{mC cm}^{-2}$ )	<sup>d</sup> $\theta_c^d$
1	624	2.58	0.08
2	1248	2.30	0.18
3	1872	2.10	0.25
4	2496	1.85	0.34
5	3120	1.62	0.42
6	3744	1.37	0.51
7	4368	1.06	0.62
8	4992	0.73	0.74

<sup>a</sup> Numbers 1-8 represent different deactivated POAP films.

<sup>b</sup> Number of potential cycles to which each POAP film was subjected in the supporting electrolyte solution (scan rate:  $0.01$   $\text{V s}^{-1}$ ).

<sup>c</sup> Voltammetric reduction charge of the different deactivated POAP films after being subjected to the number of potential cycles indicated in column 2.

<sup>d</sup> Degree of deactivation of each one of the POAP films after being subjected to the number of potential cycles indicated in column 2. The degree of deactivation was calculated from  $\theta_c^d = 1 - (Q_{\text{Red,c}}/Q_{\text{Red,T}})$ , where  $Q_{\text{Red,T}}$  ( $=2.8$   $\text{mC cm}^{-2}$ ) is the voltammetric reduction charge of a nondeactivated film.

prepared and each one of them was successively employed in an individual experiment. That is, each POAP film was subjected to a different number of potential cycles higher than 500 cycles within the potential region  $-0.2 < E < 0.5$  V in a deoxygenated supporting electrolyte solution. Then, the corresponding  $j$ - $E$  and  $\Delta R/R$ - $E$  responses for each one of the eight POAP films were recorded.

The experimental setup for simultaneous voltammetric and SR measurements on thin film electrodes has previously been described in detail [12,14]. The electrochemical cell was also the same as that described previously [14]. The electrode resistance change was measured employing the three-contact method described earlier (see Figs. 1 and 6 in [19]). In this method, the voltage drop ( $\Delta V$ ) along the resistive electrode due to a constant current ( $I_m = 1$  mA) applied to the extremes is measured. That is, in this method a current is fed through two contacts at the ends of the rectangular thin film electrode while the third one, the central contact, is connected to the current follower of the potentiostat. The possibility of coupling between the faradaic and measuring currents inside the electrode was taken into account in [19]. It was demonstrated in [19] that side effects of the faradaic current passing through the electrode can be neglected when the contacts at the ends of the electrode are symmetrically placed with respect to the central one. Then, the potential drop along the resistive electrode, together the polarization current, is measured

as a function of the applied potential  $E$ . The voltage difference at the extremes of the film is directly proportional to the resistance, and thus to the resistivity of the electrode. The potential drop  $\Delta V$  was measured with a voltmeter. The output of the voltmeter was compensated for by employing a reference tension. In this way only resistance variations,  $\Delta R$  (or  $\Delta V$  potential variations), as a function of the electrode potential,  $E$ , are measured.  $\Delta R$  changes around  $10^{-4} \Omega$  could be measured. Usually, the relative resistance change as a function of potential ( $\Delta R/R-E$ ) is recorded in SR experiments, where  $R$  is a constant value.

The use of an evaporated gold film as base electrode to deposit POAP films leads to reproducible RDEV and SR data. The good reproducibility can be attributed to the use of a smooth and renewable gold surface, obtained by evaporation, to deposit the POAP film in each experiment. In this regard, it is well-known that thin metal films obtained by evaporation (low rate of evaporation) exhibit specular surfaces with a relatively low amount of defects as compared with a massive metal surface. Thus, a metal film surface with a smooth mirrorlike finish, which is free of defects, should have a specularity parameter near 1 (for more details about the significance of  $p$  see Section 3.3.1). Our gold films are prepared at low evaporation rates and they show a specularity parameter near 0.91. With regard to the thickness of the POAP film, SEM images and permeation rate measurements reported in previous work [18] show that thick POAP films (thickness higher than 50 nm thickness) are uniform and compact enough to restrain the physical diffusion of species through the film. Also, recent resistance measurements on POAP-coated gold film electrodes [20] demonstrate the POAP coverage higher than 50 nm are sufficiently compact at the gold–POAP interface to prevent the specific adsorption of anions and cations proceeding from the external electrolyte solution on the gold film surface. However, it should be indicated that measurements at potential values slightly more negative than  $-0.30$  V are not reproducible. In this regard, at potential values more negative than  $-0.30$  V, the gold film deposited by vacuum evaporation is slowly detached (peeled off) from the gold base surface, possibly due to incipient hydrogen evolution (bubbles on the gold film surface are visible).

A PAR Model 173 potentiostat together with a PAR Model 175 function generator were also used for potentiodynamic measurements. The potential drop at the extremes of the film was measured with a Keithley Model 160 voltmeter.

### 3. Results and discussion

#### 3.1. Voltammetric responses of nondeactivated and deactivated POAP films

The voltammetric response corresponding to a nondeactivated POAP film within the potential range comprised between  $-0.2$  V and  $0.5$  V is shown in Fig. 1 (plot (a)). As was indicated, the POAP film maintains this response with potential cycling within the potential range  $-0.2$  V  $< E < 0.5$  V up to 500 potential cycles (scan rate  $0.01$  V  $s^{-1}$ ). However, after a higher number of potential cycles this response start to change. Fig. 1 compares the  $j$ - $E$  responses of a nondeactivated POAP film (plots (a)) with those of the films (5), (7) and (8) (see first column of Table 1) that were subjected to the corresponding number of potential cycles ( $>500$ ) indicated in column 2 of Table 1. The more attenuated voltammetric response observed in Fig. 1, as the number of potential cycles increases indicates a deactivation of the POAP film. In this regard, voltammetric reduction charge values corresponding to the completely reduced POAP films were compared for a nondeactivated film ( $Q_{\text{Red,T}} = 2.8$  mC  $\text{cm}^{-2}$ ) and the different deactivated films ( $Q_{\text{Red,c}}$ ) indicated in

Table 1. Then, a degree of deactivation (column 4 of Table 1) was defined as

$$\theta_c^d = 1 - (Q_{\text{Red,c}}/Q_{\text{Red,T}}) \quad (1)$$

$Q_{\text{Red,c}}$  is the total reduction charge assessed by integration of the corresponding  $j$ - $E$  response from  $E = 0.5$  V towards the negative potential direction for a deactivated film, and  $Q_{\text{Red,T}} = 2.8$  mC  $\text{cm}^{-2}$  is the total reduction charge for the nondeactivated film. In this way, for a nondeactivated POAP film (plot (a) in Fig. 1) the degree of deactivation was  $\theta_c^d = 0$ , taking  $Q_{\text{Red,T}} = 2.8$  mC  $\text{cm}^{-2}$  as reference charge. However, values of  $\theta_c^d > 0$  are indicative of POAP films that have been deactivated.

#### 3.2. Rotating disc electrode voltammetry measurements in the presence of the hydroquinone/*p*-benzoquinone redox couple

As was indicated, RDEV was employed to study the behaviour of nondeactivated and deactivated POAP films in contact with an electroactive solution containing the hydroquinone/*p*-benzoquinone redox couple. In the presence of a redox active solution, besides charge transfer between redox sites of the polymer and the external redox couple, the oxidation and reduction of fixed sites introduce charged sites into the polymer film, which, in order to achieve charge neutrality, require the ingress of counterions from the contacting electrolyte solution and, according to the Donnan relation, the egress of co-ions. Disregarding the charge-transport control, a redox polymer undergoing electrolysis may follow Fick's diffusion law and usually Fick's formalism agrees with the experimental results. Electron hopping is believed to be the mechanism for electron transport at polymer materials, but it is also possible that ion motions may partially or totally control the rate of charge transport. Then, steady-state current–potential curves were interpreted on the basis of the traditional electron hopping model [21–23].

In previous work [18] RDEV experiments at gold electrodes coated with POAP films were carried out to study the diffusion processes of benzoquinone (Q) and hydroquinone (HQ) species through nondeactivated films. Diffusion-limited currents at  $E < 0.0$  V for Q reduction and at  $E > 0.8$  V for HQ oxidation were observed. While the anodic limiting current corresponds to the oxidation of HQ species that penetrate through the polymer film to reach the metal surface, cathodic limiting currents for Q reduction are related to a rapid electron-transfer mediation at the POAP|redox active solution interface, which occurs without significant penetration of Q into the polymer layer. In order to analyze the effect of the PPC on the electron conduction at POAP, only the electrochemical behaviour of nondeactivated and deactivated POAP films at negative potential values ( $E < 0.0$  V) was considered.

Fig. 2 shows stationary current–potential curves ( $I$ - $E$ ) at different electrode rotation rates,  $\Omega$ , for a nondeactivated POAP film contacting a  $0.1$  M  $\text{HClO}_4 + 0.4$  M  $\text{NaClO}_4 + 2 \times 10^{-3}$  M Q/HQ solution. ( $I$ - $E$ ) curves at different  $\Omega$  values were also obtained for each one of the deactivated POAP films indicated in Table 1. For instance, Fig. 3 shows this representation for a POAP film with  $\theta_c^d = 0.51$ . As can be seen by comparing Figs. 2 and 3, at each electrode rotation rate, both anodic and cathodic limiting currents for a deactivated POAP film are lower than those for a nondeactivated one. Also, after a given electrode rotation rate, which depends on the degree of deactivation, the cathodic limiting current for a deactivated film becomes independent of this variable.  $I_{\text{lim,c}}$  versus  $\Omega^{1/2}$  dependences at potential values  $E < 0.0$  V for both nondeactivated and deactivated POAP films are shown in Fig. 4. For a nondeactivated POAP film a linear  $I_{\text{lim,c}}$  versus  $\Omega^{1/2}$  dependence, which follows the Levich equation, is obtained within a wide range of  $\Omega$  values.

However, for POAP films that have been deactivated, after a certain  $\Omega$  value, a constant cathodic limiting current value,  $I_{lim,c}$ , independent of  $\Omega$  is achieved. Also, it is observed that the transition at which the cathodic limiting current becomes independent of  $\Omega$  occurs at lower  $\Omega$  values as the degree of deactivation increases. The explanation of this effect can be given in terms of the electron hopping model [21-23]. Limiting current values at which  $I_{lim,c} (= I_e)$  becomes constant were considered as a representation of the maximum flux of electrons confined in the polymer, according to Eq. (2) [23].

$$I_e = nFAD_e c / \phi_p \quad (2)$$

In Eq. (2),  $c$  is the concentration of redox sites of the polymer and  $\phi_p$  the polymer film thickness.  $D_e$  represents a measure of the electron hopping rate and  $n$  expresses the numbers (fractions) of unit charges per monomer unit of the polymer.  $A$  is the electrode area and  $F$  the Faraday's constant. Experimental  $I_e$  values, corresponding to each one of the eight deactivated POAP films contacting a  $2 \times 10^{-3}$  M HQ/Q solution, were extracted from the cathodic plateau and they are listed as a function of  $\theta_c^d$  in Table 2. As can be seen from Table 2,  $I_e$  decreases with increasing  $\theta_c^d$ . In this regard, such a constant value of the current ( $I_e$ ) at a given  $\Omega$  value for deactivated POAP films can be related to a slow electron transport across the POAP film to mediate in the electron-transfer reaction at the polymer|solution interface, as compared with a nondeactivated POAP film. As one increases the flux of Q (increase of  $\Omega$ ) from the bulk solution, then if the flux exceeds the supply of electrons from the electrode through the polymer to the electrolyte interface, the rate-limiting step will shift from the limiting transport of Q to the limiting transport of the charge through the polymer. It is found that the constant current for a given deactivated film remains unchanged with changing redox couple concentration in solution. That is, even though the  $I_{lim,c}$  versus  $\Omega^{1/2}$  slope increases with the increase of the HQ/Q concentration, the constant current value  $I_e$  for a given deactivated film, remains unchanged. Obviously, the constant current value is observed at a lower electrode rotation rate value as the HQ/Q concentration increases. According to Eq. (2), the slower electron transport in deactivated films, as compared with nondeactivated ones, could be attributed to a decrease of  $D_e$ . By employing the  $I_e$  values shown in Table 2 and using the parameter values  $c = 4.7$  M [1],  $A = 1$  cm<sup>2</sup>,  $n = 0.44$  [24] and

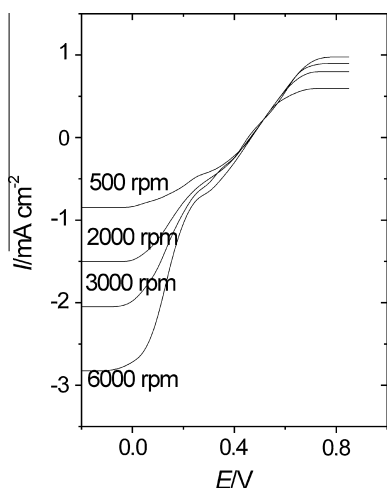


Fig. 2. Steady-state current-potential ( $I$ - $E$ ) curves for different rotation rates ( $\Omega$ ) of the rotating disc electrode. A nondeactivated POAP film.  $\Omega$  Values are indicated in the figure. Film thickness: 60 nm. Electrolyte: 0.1 M HClO<sub>4</sub> + 0.4 M NaClO<sub>4</sub> +  $2 \times 10^{-3}$  M (HQ/Q).

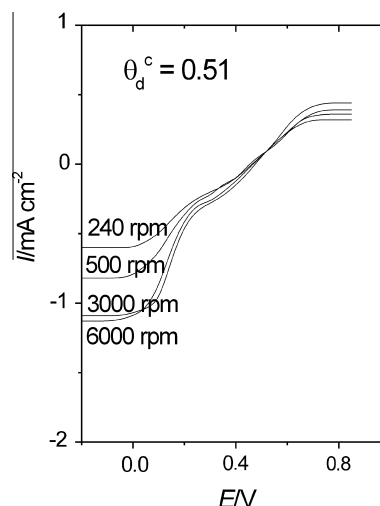


Fig. 3. Steady-state current-potential ( $I$ - $E$ ) curves for different rotation rates ( $\Omega$ ) of the rotating disc electrode. A deactivated POAP film ( $\theta_c^d = 0.51$ ).  $\Omega$  values are indicated in the figure. Film thickness: 60 nm. Electrolyte: 0.1 M HClO<sub>4</sub> + 0.4 M NaClO<sub>4</sub> +  $2 \times 10^{-3}$  M (HQ/Q).

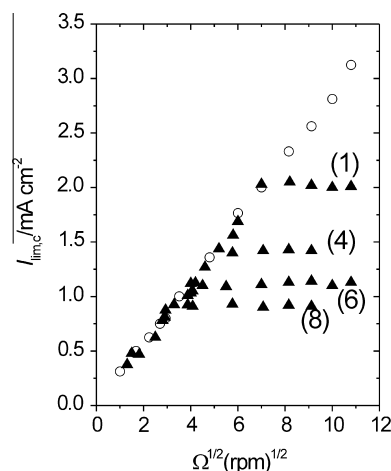


Fig. 4. Levich representations  $I_{lim,c}$  versus  $\Omega^{1/2}$  for POAP films contacting a 0.1 M HClO<sub>4</sub> + 0.4 M NaClO<sub>4</sub> +  $2 \times 10^{-3}$  M (HQ/Q) solution. (O) A nondeactivated POAP film. (1), (4), (6) and (8) correspond to the four films indicated in Table 1.

$\phi_p = 60$  nm in Eq. (2), one obtains a decrease of  $D_e$  from  $6.01 \times 10^{-11}$  to  $2.76 \times 10^{-11}$  cm<sup>2</sup> s<sup>-1</sup> for a relative increase of  $\theta_c$  from 0.08 to 0.74.

The electron diffusion coefficient,  $D_e$ , in electroactive materials has been expressed in terms of the mean distance between adjacent active redox sites [25], according to  $D_e = (a^2 k_o)$ , where  $k_o$  is the intermolecular electron-transfer rate constant and  $a$  is the mean distance between two adjacent redox sites. The hopping rate,  $k_o$ , exhibits an exponential dependence on  $a$ , through the energy  $-U(x+a)$  of a state with an electron in the position  $x$  along the current direction (see Eq. (23) in Ref. [25]). In this respect, a  $k_o$  decrease should be expected as the hopping distance  $a$  increases. The decrease of  $D_e$  obtained from Eq. (2) could be attributed to an increase of the hopping distance between remnant active redox sites after deactivation.

It is interesting to remark that a constant current  $I_e$  independent of  $\Omega$  is also obtained for a nondeactivated POAP film in contact with a 0.1 M HClO<sub>4</sub> + 0.4 M NaClO<sub>4</sub> +  $2 \times 10^{-3}$  M Q/HQ solution. However, in this case the constant current is obtained at very high electrode rotation rates ( $\Omega > 8000$  rpm). It is possible that at high

**Table 2**  
Electron current  $I_e$  as a function of the degree of deactivation  $\theta_c^d$  of a POAP film.

<sup>a</sup> POAP films	<sup>b</sup> $\theta_c^d$	<sup>c</sup> $I_e$ (mA cm <sup>-2</sup> )
1	0.08	2.02
2	0.18	1.64
3	0.25	1.46
4	0.34	1.40
5	0.42	1.21
6	0.51	1.12
7	0.62	0.98
8	0.74	0.92

<sup>a</sup> Numbers 1–8 represent different deactivated POAP films.

<sup>b</sup> Degree of deactivation of each one of the POAP films after being subjected to the potential number of cycles indicated in column 2 of Table 1.

<sup>c</sup> Electron current  $I_e$  as a function of the degree of deactivation,  $\theta_c^d$  obtained by RDEV in the presence of the HQ/Q redox couple.

angular speeds of the rotating disc electrode, the flux into the bulk solution would not longer laminar, so that the proportionality between the current and  $\Omega^{1/2}$ , should not be expected. However, if the HQ/Q concentration is increased (0.01 M) a constant current  $I_e$  ( $\approx 15$  mA cm<sup>-2</sup>) is observed for a nondeactivated film at about 7000 rpm (Fig. 5). As this value is reproducible and it decreases as the deactivation of the polymer increases, then our interpretation of a change in the rate limiting process during the mediated electron-transfer reaction seems to be correct. Similar effects were observed for other polymers [26]. Considering the constant current value obtained for high HQ/Q concentrations, a  $D_e$  about  $1.22 \times 10^{-10}$  cm<sup>2</sup> s<sup>-1</sup> is obtained for a nondeactivated POAP film. This finding seems to indicate that a restriction for the electron transport also occurs across a nondeactivated POAP film in contact of a concentrated electroactive solution and high enough flux into the bulk solution.

The loss of electroactivity of a polymer film under continuous potential cycling has been attributed to an excessive uptake of doping sites by dopant anions from the external electrolyte solution. Then, after a great number of potential cycles, anions may associate strongly with positive sites of the polymer chains resulting in electrostatic cross-linking, which in turn leads to the polymer deactivation [27,28]. However, the prolonged potential cycling can also alter the molecular structure of a POAP film, and hence, its physical properties. Thus, the diffusion coefficient obtained in this work from RDEV could not be a real physical property of the polymer. However, values obtained for nondeactivated and

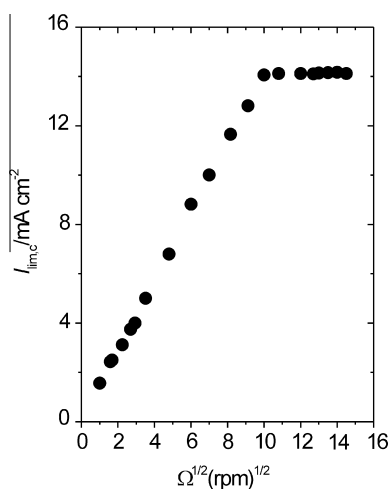


**Fig. 5.** Levich representation  $I_{lim,c}$  versus  $\Omega^{1/2}$  for a nondeactivated POAP film contacting a 0.1 M HClO<sub>4</sub> + 0.4 M NaClO<sub>4</sub> + 0.01 M (HQ/Q) solution.

deactivated POAP films allows one, at least, to compare the behaviours of films before and after they have been subjected to an extensive potentiodynamic cycling.

### 3.3. Surface resistance measurements

Experiments employing a nontraditional technique, the surface resistance (SR), were carried out in this work in order to study POAP deactivation. It is interesting to remark that unlike other techniques, which is based on complicated models, the SR technique is based on a simple electron dispersion model [29,30]. The SR technique is sensitive to the distribution of scatterers at a metal film surface [12]. In previous work it was proved that SR is a useful technique to detect changes in the redox site distribution during the redox switching of a POAP film deposited on a thin gold film [15,31]. However, as the SR technique may be considered as a non-traditional approach in electrochemistry, a brief explanation about the interpretation of the resistance changes exhibited by a thin metal film coated with an electroactive polymer film is given in the next paragraphs.

#### 3.3.1. Electronic transport in thin metal films

Electronic transport in thin metal films is strongly affected by interfacial phenomena. For example, the scattering of conduction electrons at planar interfaces defined by the top and bottom surfaces of the film under study can contribute significantly to the resistivity. In the case of thin metal films, the electrical resistivity,  $\rho_f$ , is higher than the bulk resistivity,  $\rho_m$ , of the massive metal of the same structure as the metal film and the  $\rho_f/\rho_m$  ratio decreases with increasing the film thickness,  $\phi_m$ . This “size effect” becomes evident when  $\phi_m$  is comparable with the mean free path,  $l_m$ , of the conduction electrons. The theory to account for the size effect was postulated by Fuchs [29] and Sondheimer [30]. The exact expression for the dependence of the film resistivity,  $\rho_f$ , as a function of  $\phi_m$  is complicated. However, it can be reduced to a limiting form when  $\phi_m/l_m \geq 1$ :

$$\rho_f/\rho_m = 1 + (3/8)(1 - p)l_m/\phi_m \quad (3)$$

In Eq. (3),  $p$  is the specularity parameter [30]. This parameter represents the probability of an electron being reflected specularly or diffusely at the film surface. The  $p$  value ranges from 0 for complete diffuse scattering to 1 for complete specular scattering. At first, it should be considered that thin metal films can be prepared to satisfy the Fuch’s model in a sufficient way to exhibit a specularity parameter near 1 (a surface with a smooth mirrorlike finish that is free of defects). However, this parameter, which is also interpreted as the fraction of the surface that specularly reflects electrons, depends on the quality of the metal film surface, that is, on the method of preparation of the metal film [32]. In this sense, an appreciable fraction of the conduction electrons can be scattered diffusely and give rise to an additional resistance, which correlates with the roughness of surface topography and the presence of surface defects. All these imperfections should lead to experimental  $p$  values lower than 1. As was indicated in the experimental section, our gold films are prepared at low evaporation rates and they show a specularity parameter near 0.91.

Besides the factors mentioned above, if foreign entities are present on the film surface, translational symmetry parallel to the interface, changes and additional scattering of the conduction electrons occurs. This electron dispersion effect, brought about by the presence of entities on the metal surface, thereby acting as dispersion centres for the surface reflection of the electrons from the inside of the metal, has been analyzed on the basis of Eq. (3). Assuming that the specularity,  $p$ , is the principal parameter influenced by the surface concentration of foreign scattering centres

at the film surface  $\Gamma_{\text{surf}}$ , differentiation of Eq. (3) leads to the relationship:

$$\Delta\rho_f = -3/8(\rho_m I_m / \phi_m)(\Delta p) \quad (4)$$

On the assumption that the increase of  $\Gamma_{\text{surf}}$  increases the diffuse scattering of the electrons,  $\Delta p = -k\Gamma_{\text{surf}}$ , an increase in  $\Delta\rho_f$  would be expected with increasing  $\Gamma_{\text{surf}}$  (Eq. (4)). In terms of the resistance changes ( $\Delta R = \Delta\rho_f G / \phi_m$ ), Eq. (4) can be written as:

$$\Delta R = -3/8G(\rho_m I_m / \phi_m^2)\Delta p \quad (5)$$

### 3.3.2. The POAP-coated gold film electrode

As was described in the experimental section, POAP was deposited on a thin gold film electrode whose thickness was of the order of the mean free path of conduction electrons of gold and SR was employed to investigate changes in the electronic properties at the gold/POAP interface during deactivation of the polymer. Simultaneous voltammetric and SR responses corresponding to a nondeactivated POAP film within the potential range comprised between  $-0.2$  V and  $0.5$  V are shown in Fig. 6. As was indicated, the POAP film maintains these responses with potential cycling within the potential range  $-0.2$  V  $< E < 0.5$  V up to 500 potential cycles (scan rate  $0.01$  V  $s^{-1}$ ). However, after a higher number of potential cycles, these responses start to change. The evolution of the  $\Delta R/R$  versus  $E$  response for a 60 nm thick POAP film with PPC is shown in Fig. 7. Simultaneously with the  $\Delta R/R$  versus  $E$  response, the evolution of the voltammetric response was also recorded for each POAP film. As the electrode area and the thickness of the POAP films employed in SR were the same as those used in CV and RDEV measurements, the evolution of the voltammetric response with PPC was practically the same as that shown in Fig. 1.

With regard to  $\Delta R/R$  versus  $E$  response, the potential drop along the thin gold film electrode was compensated for at the reduced state of POAP ( $E = -0.2$  V) (see experimental section). Then, an increase in the SR of the POAP-coated gold electrode is recorded in going from  $-0.2$  V to  $0.5$  V. The increase of the gold film resistance during the transition from the reduced state to the oxidized state of a nondeactivated POAP film (Fig. 6) was explained in terms of the generation of electronic entities at the polymer chains near the electrode surface, which occurs by electron transfer across the polymer/metal interface [12]. With respect to the polymer redox conversion at the gold film surface, one has to keep in mind

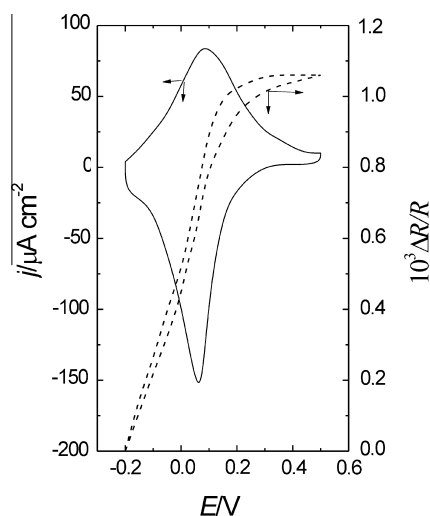


Fig. 6. Simultaneous  $\Delta R/R$ - $E$  and  $j$ - $E$  responses of a 30 nm thick gold film coated with a  $2.8$  mC  $cm^{-2}$  ( $\phi_p = 60$  nm) thick POAP film. Electrolyte:  $0.1$  M  $HClO_4 + 0.4$  M  $NaClO_4$ . Scan rate:  $\nu = 0.01$  V  $s^{-1}$ .

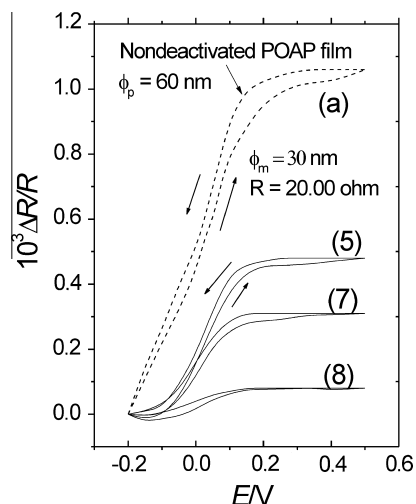
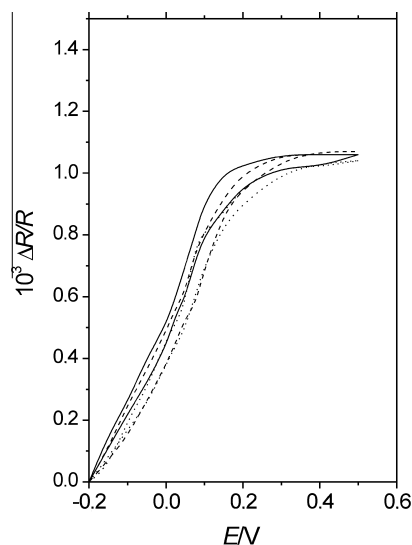


Fig. 7.  $\Delta R/R$ - $E$  responses obtained simultaneously with the ( $j$ - $E$ ) responses shown in Fig. 1. The same notation and conditions as in Fig. 1 have been used. Thickness of the gold film  $\phi_m = 30$  nm, resistance value of the gold film,  $R = 20.02$   $\Omega$ . Thickness of the POAP film,  $\phi_p = 60$  nm. Electrolyte:  $0.1$  M  $HClO_4 + 0.4$  M  $NaClO_4$ . Scan rate:  $\nu = 0.01$  V  $s^{-1}$ .

that the resistance changes at metal films are not the direct result of the electron transfer between the species on the metal film surface and the metal, but they rather originate from the effect of foreign surface entities on the conduction electrons of the metal itself. On the other hand, as the potential drop along the resistive electrode ( $R \sim 20.02$   $\Omega$  for  $\phi_m = 30$  nm) due to the measuring current  $I_m$  (see experimental section) is compensated for, only  $\Delta R$  changes associated with interfacial phenomena are recorded. Thus, the measured resistance change for a POAP-coated gold film electrode is only related to an interfacial (metal/polymer) electron dispersion process occurring during the reduction-oxidation process of the polymer film. In this regard, Fig. 8 shows that by increasing the POAP film thickness between 50 nm and 69 nm, the  $\Delta R/R$  change remains practically the same. Obviously, the voltammetric responses (not shown) depend on the POAP thickness.

According to Eq. (5), the  $\Delta R/R$  increase in going from  $E = -0.2$  V to  $E = 0.5$  V in Fig. 6 can be attributed to a  $p$  decrease. The redox switching of POAP was interpreted in terms of the oxidation of the amino groups to imine [6]. Then, the increase of  $\Delta R/R$  during POAP oxidation can be explained in terms of an interfacial distribution of scatterers (imine sites) in the oxidized state with a spacing among them larger than that corresponding to amine sites in the reduced state [6,12]. That is, the distribution of imine species in the oxidized state of POAP should be less compact than the corresponding distribution of amine species in the reduced state, which should lead to a more diffuse reflection of conduction electrons at the gold/POAP interface (lower specularly parameter at the oxidized state as compared with the value at the reduced one,  $p_{\text{ox}} < p_{\text{red}}$ ) [12]. A confirmation that supports a more extended configuration of oxidized sites, as compared with that of reduced ones, at POAP can be given in terms of gaps, which appear during POAP oxidation. In this respect, optical measurements on POAP films reveal that only one in every four or five amine sites is converted to the corresponding imine site [6]. Thus, the existence of inactive gaps within the distribution of oxidized sites of POAP could justify that POAP in its oxidized state reflects conduction electrons of gold more diffusely than in its reduced state. Further confirmation about the different reflecting properties of the oxidized and reduced states of POAP can be found in the different values of the site interaction parameters ( $r$ ) obtained from the cathodic and anodic voltammetric response of POAP. A nonideal behaviour of POAP, which is actually expected considering the rather high



**Fig. 8.**  $\Delta R/R$ - $E$  responses of a nondeactivated POAP films deposited on a 30 nm thick gold film. Thicknesses of the POAP films: (---)  $\phi_p = 69$  nm; (—)  $\phi_p = 60$  nm; (···)  $\phi_p = 52$  nm. Electrolyte: 0.1 M HClO<sub>4</sub> + 0.4 M NaClO<sub>4</sub>. Scan rate:  $\nu = 0.01$  V s<sup>-1</sup>.

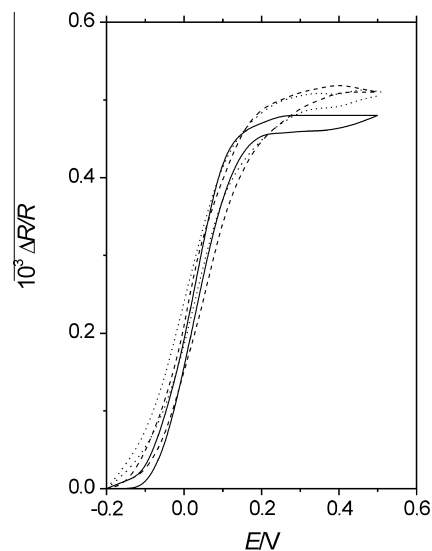


**Fig. 9.**  $\Delta R/R$ - $E$  responses of a deactivated POAP film ( $\theta_d = 0.42$ ) deposited on a 30 nm thick gold film. Thicknesses of the POAP films: (---)  $\phi_p = 69$  nm; (—)  $\phi_p = 60$  nm; (···)  $\phi_p = 52$  nm. Electrolyte: 0.1 M HClO<sub>4</sub> + 0.4 M NaClO<sub>4</sub>. Scan rate:  $\nu = 0.01$  V s<sup>-1</sup>.

concentration of active sites in the film (i.e.,  $c = 4.7$  M [1,2]), leads to the following values of anodic and cathodic site interaction parameters:  $r_a = -0.55$  M<sup>-1</sup> and  $r_c = -0.18$  M<sup>-1</sup>, respectively. Both are negative, thus involving a repulsive energy of interaction. As a higher repulsion is observed between oxidized sites than between reduced ones at POAP, a more extended configuration of oxidized sites should be expected as compared with the corresponding distribution of reduced sites.

With regard to POAP deactivation, as can be seen from Fig. 7, the more deactivated the POAP film becomes, the more attenuated the  $\Delta R/R$  change is in going from the reduced to the oxidized state of POAP. As was indicated, the measured resistance change is only related to an interfacial (metal/polymer) electron dispersion process that occurs during reduction-oxidation of the polymer film. This fact was also proved for deactivated films by changing the POAP film thickness. Figs. 9 and 10 show that by increasing the POAP film thickness between 50 nm and 69 nm, the  $\Delta R/R$  change for a deactivated film, remains practically the same.

According to Eq. (5), the  $\Delta R/R$  versus  $E$  change, at constant POAP film thickness, depends on the gold film thickness. That is, the thinner the gold film is, the higher the  $\Delta R$  value is, and then, the more pronounced the resistance  $\Delta R/R$  change becomes. This fact can be seen by comparing Fig. 7 with Fig. 11. Despite the absolute resistance value,  $R$  increases as the metal film thickness decreases, the interfacial effects in the  $\Delta R/R$  change become magnified as the thickness of the gold film decreases. In this regard, the lower the metal film thickness is, the more sensitive the SR technique becomes to study interfacial phenomena. This effect is quantitatively shown in Fig. 12, where the  $\Delta R/R$  change in going from  $-0.2$  V to  $0.5$  V is represented as a function of the degree of deactivation of the POAP film for three different gold film thicknesses.

The specularity parameter change ( $\Delta p$ ) in going from the reduced to the oxidized states of POAP at each degree of deactivation can be obtained from Eq. (5). The  $\Delta p$  versus  $\theta_d$  dependences for the three different gold film thicknesses indicated in Fig. 12 are shown in Fig. 13. The following values were employed in Eq. (5) to calculate  $\Delta p$ :  $l_m$  ( $= 22$  nm at  $25^\circ\text{C}$ ) is the mean free path of the conduction electrons of gold,  $\rho_m$  ( $= 2.4 \times 10^{-6}$  Ω cm) is the bulk resistivity of the massive metal (gold) of the same structure as the metal film,  $\phi_m$  is the thickness of the metal film,  $G$  ( $= 2.043$ ) is the relationship between the length,  $l$ , and the width,

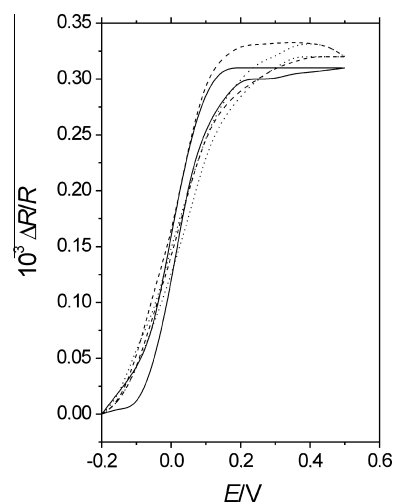


**Fig. 10.**  $\Delta R/R$ - $E$  responses of a deactivated POAP film ( $\theta_d = 0.62$ ) deposited on a 30 nm thick gold film. Thicknesses of the POAP films: (---)  $\phi_p = 69$  nm; (—)  $\phi_p = 60$  nm; (···)  $\phi_p = 52$  nm. Electrolyte: 0.1 M HClO<sub>4</sub> + 0.4 M NaClO<sub>4</sub>. Scan rate:  $\nu = 0.01$  V s<sup>-1</sup>.

$w$ , of the rectangular gold film on which the POAP film was deposited. The resistance values,  $R$ , of the gold films are experimentally obtained. As was indicated,  $\Delta p$  is always negative, that is,  $p_{\text{ox}} < p_{\text{red}}$ . The maximal difference in the reflecting properties of the POAP/gold interface for the conduction electron of gold between the oxidized and the reduced states of POAP occurs for a nondeactivated POAP film; however, the reflecting properties of the POAP/gold interface at the reduced and oxidized states of POAP tend to match as the degree of deactivation increases. As can be seen from Fig. 13, again the lower the thickness of the gold film is, the more pronounced the  $\Delta p$  change at the gold/POAP interface at each degree of deactivation becomes.

The gradual attenuation of the  $\Delta p$  versus  $\theta_d$  dependences shown in Fig. 13 seems to be indicative of a redox site distribution of the POAP film (scatterers for the conduction electrons of the gold film) that changes as the degree of deactivation of the polymer increases. In this regard, the distribution of scatterers at the gold/

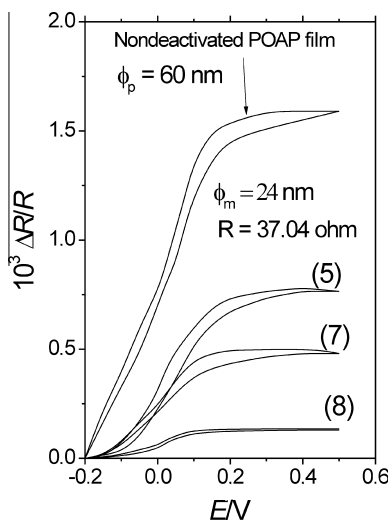


**Fig. 11.**  $\Delta R/R$ -E responses of a POAP-coated gold film electrode. Thickness of the POAP film,  $\phi_p = 60$  nm. Thickness of the gold film  $\phi_m = 24$  nm, resistance value of the gold film,  $R = 37.04 \Omega$ . (a) A nondeactivated POAP film ( $\theta_c^d = 0$ ). Curves (5), (7) and (8) correspond to films whose degree of deactivation is:  $\theta_c^d = 0.42$ ;  $\theta_c^d = 0.62$  and  $\theta_c^d = 0.74$ , respectively. Electrolyte: 0.1 M  $\text{HClO}_4$  + 0.4 M  $\text{NaClO}_4$ . Scan rate:  $\nu = 0.01 \text{ V s}^{-1}$ .

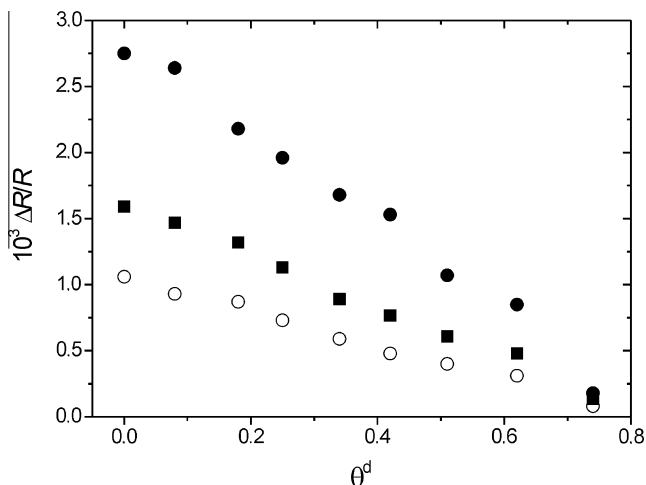


**Fig. 12.**  $\Delta R/R$  change in going from the reduced to the oxidized state of POAP as a function of the degree of degradation,  $\theta_c^d$ . Thickness of the POAP film,  $\phi_p = 60$  nm. Thickness of the gold film,  $\phi_m$ : (○) 30 nm; (■) 24 nm; (●) 17 nm.

POAP interface for a POAP film with a high enough degree of deactivation shows no difference for the reflection of the conduction electrons of the gold film in going from the reduced to the oxidized state of the POAP film. This finding could be related to the decrease of the diffusion coefficient with the increase of the degree of deactivation of the POAP film obtained from steady-state current-potential curves at the reduced state of the polymer. As was indicated, the decrease of the diffusion coefficient with the polymer deactivation can be explained in terms of an increase in the hopping distance between redox sites with the increase of the degree of deactivation of POAP. Unfortunately RDEV measurements at the anodic plateau of POAP show that anodic limiting current ( $E > 0.8 \text{ V}$ ) corresponds to the oxidation of HQ species that penetrate through the polymer film to reach the metal surface, and then, it was not possible to obtain the dependence of the diffusion coefficient for the charge transport process at the oxidized state of POAP on the degree of deactivation.

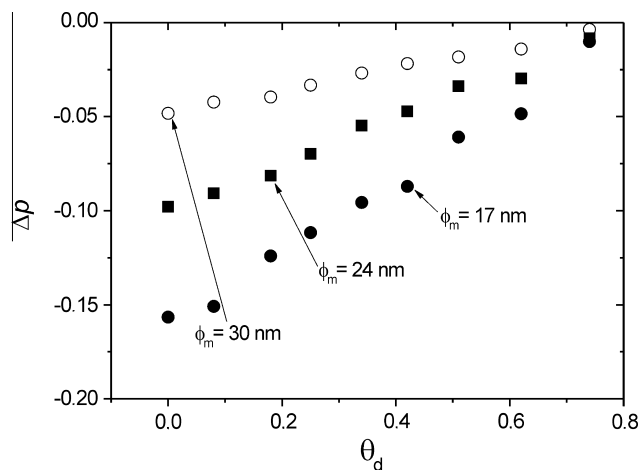


**Fig. 13.** The  $\Delta\rho$  versus  $\theta_d$  dependence for the different gold film thicknesses:  $\phi_m = 30$  nm;  $\phi_m = 24$  nm;  $\phi_m = 17$  nm. The corresponding resistances are:  $R = 20.02 \Omega$ ;  $R = 37.04 \Omega$ ;  $R = 78.11 \Omega$ .

#### 4. Conclusions

In this work it is demonstrated that poly(o-aminophenol) films maintain their conducting properties unaltered for about 500 potential cycles within the potential range  $-0.2 < E < 0.5 \text{ V}$  (SCE) at a scan rate of  $0.010 \text{ V s}^{-1}$ . However, a loss of conductivity was observed as the number of potential cycles was extended beyond 500. The loss of conductivity of POAP with prolonged potential cycling is demonstrated by the attenuation of the voltammetric response, the decrease of a charge transport parameter obtained from RDEV and the gradual attenuation of the surface resistance change in going from the reduced to the oxidized states of POAP. The attenuation of the surface resistance change as the degree of deactivation of POAP increases was attributed to a change in the redox site configuration, which seems to be consistent with the increase in the electron hopping distance between redox sites proposed to explain the decrease of the diffusion coefficient value obtained from RDEV measurements.

#### Acknowledgements

The author gratefully acknowledges the Consejo Nacional de Investigaciones Científicas y Técnicas (CONICET) and also the Facultad de Ciencias Exactas, National University of La Plata (UNLP).

#### Appendix A. Supplementary material

Supplementary data associated with this article can be found, in the online version, at <http://dx.doi.org/10.1016/j.jelechem.2014.01.023>.

#### References

- [1] C. Barbero, J.J. Silber, L. Sereno, J. Electroanal. Chem. 291 (1990) 81–101.
- [2] C. Barbero, J.J. Silber, L. Sereno, J. Electroanal. Chem. 263 (1989) 333–352.
- [3] T. Ohsaka, S. Kunimura, N. Oyama, Electrochim. Acta 33 (1988) 639–645.
- [4] R. Tucceri, P.M. Arnal, A.N. Scian, Can. J. Chem. 91 (2013) 91–112.
- [5] D. Scolari, R. Tucceri, Micro Nanosystems 3 (2011) 115–130.
- [6] R.I. Tucceri, C. Barbero, J.J. Silber, L. Sereno, D. Posadas, Electrochim. Acta 42 (1997) 919–927.
- [7] O. Levin, V. Kondratiev, V. Malev, Electrochim. Acta 50 (2005) 1573–1585.
- [8] M.C. Miras, A. Badano, M.M. Bruno, C. Barbero, Portugaliae Electrochim. Acta 21 (2003) 235–243.
- [9] J. Yano, H. Kawakami, S. Yamasaki, Y. Kanno, J. Electrochem. Soc. 148 (2001) E61–E65.
- [10] M.J. Lobo, A.J. Miranda, J.M. López-Fonseca, P. Tuñón, Anal. Chim. Acta 325 (1996) 33–42.



- [11] A.Q. Zhang, C.Q. Cui, J.Y. Lee, *J. Electroanal. Chem.* 413 (1996) 143–151.
- [12] R. Tucceri, *Surf. Sci. Rep.* 56 (2004) 85–157.
- [13] R.I. Tucceri, D. Posadas, *J. Electroanal. Chem.* 191 (1985) 387–399.
- [14] R.I. Tucceri, D. Posadas, *J. Electrochem. Soc.* 130 (1983) 104–107.
- [15] R.I. Tucceri, *J. Electroanal. Chem.* 505 (2001) 72–84.
- [16] K.L. Chopra, *Thin Film Phenomena*, McGraw-Hill Co., New York, 1969.
- [17] C. Barbero, J. Zerbino, L. Sereno, D. Posadas, *Electrochim. Acta* 32 (1987) 693–697.
- [18] A. Bonfranceschi, A. Pérez Córdoba, S. Keunchkarian, S. Zapata, *J. Electroanal. Chem.* 477 (1999) 1.
- [19] R.I. Tucceri, D. Posadas, *J. Electrochem. Soc.* 128 (1981) 1478–1483.
- [20] R. Tucceri, *J. Surf. Eng. Mater. Adv. Technol.* 3 (2013) 205–216.
- [21] C.P. Andrieux, J.M. Savéant, *J. Electroanal. Chem.* 111 (1980) 377–381.
- [22] E. Laviron, *J. Electroanal. Chem.* 112 (1980) 1–9.
- [23] C. Deslouis, B. Tribollet, in: H. Gerischer, C. Tobias (Eds.), *Advances in Electrochemical Science and Engineering*, vol. 2, VCH Publishers, New York, USA, 1992, p. 205.
- [24] C. Barbero, R.I. Tucceri, D. Posadas, J.J. Silber, L. Sereno, *Electrochim. Acta* 40 (1995) 1037–1040.
- [25] Ch.E.D. Chidsey, R.W. Murray, *J. Phys. Chem.* 90 (1986) 1479–1484.
- [26] W.J. Albery, M.G. Boutelle, A.R. Hillman, *J. Electroanal. Chem.* 182 (1985) 99–111.
- [27] P. Novák, K. Müller, K.S.V. Santhanam, O. Haas, *Chem. Rev.* 97 (1997) 207–281.
- [28] Z. Cai, R. Martin, *J. Electroanal. Chem.* 300 (1991) 35.
- [29] F. Fuchs, *Proc. Camb., Phyl. Soc. Math. Phys. Sci.* 34 (1938) 100.
- [30] E.H. Sondheimer, *Adv. Phys.* 1 (1952) 1.
- [31] R.I. Tucceri, *J. Electroanal. Chem.* 543 (2003) 61–71.
- [32] F.M. Romeo, R.I. Tucceri, D. Posadas, *Surf. Sci.* 203 (1988) 186–200.